USING STABLE ISOTOPES OF PLANT LEAF WAXES FROM SONORAN DESERT NATIVES TO UNDERSTAND PLANT LIFE HISTORIES ON AN ANNUAL SCALE

By

MIKAYLA KAYLEIGHEN GERDES

_____

A Thesis Submitted to The Honors College

In Partial Fulfillment of the Bachelors degree
With Honors in

Biology

THE UNIVERSITY OF ARIZONA

M A Y 2 0 1 8

Approved by:

_____

Dr. Jessica Tierney
Department of Geoscience

ABSTRACT

As climate change alters the Sonoran Desert, it is important to understand carbon movement within this unique ecosystem. Serving as one of the first known studies of its kind, this study uses carbon isotope fractionation tracers to investigate annual life histories of four key Sonoran Desert plant species that have evolved to incorporate either C_3 or C_4 photosynthetic mechanisms: *Prosopis velutina* (velvet mesquite), *Olneya tesota* (ironwood), *Simmondsia chinensis* (jojoba), and *Aristida ternipes* (spidergrass). Wax *n*-alkane chain-length distributions (average chain length, ACL; and carbon preference index, CPI) as well as *n*-alkane carbon isotopic composition ($\delta^{13}C$) are analyzed to study how plants alter their waxy leaf coatings through the seasonal cycle in response to water stress and the growing seasons. C_3 plants had an average leaf tissue $\delta^{13}C$ value of -31.0‰ and C_4 plants had an average value of -26.6‰. $\delta^{13}C$ anomalies also show a greater enrichment of ^{13}C in C_4 plants, demonstrating C_4 plants respond more readily to seasonal variability and precipitation events, in comparison. Overall, this study serves to provide possible implications for the role of an arid environment on plant *n*-alkane distributions within the Sonoran Desert Region.

INTRODUCTION

Anthropogenic carbon emissions have given rise to great concern for future climatic conditions and their possible effects on biomes and their inhabitants. As emissions continue to play a role in altering atmosphere composition and worldwide carbon fluxes, there has become a definitive need for understanding how carbon movement can impact plant life histories, not only in present conditions, but future conditions as well. Plants are useful in studying how climate change will impact the world's biomes and ecosystems because they are rooted in place and must be specifically adapted to particular areas of interest in order to inhabit those areas. Thus, in many cases, plants are often considered endemic to a particular biome or ecosystem. Due to their special adaptability to a particular area, and their inability to move, plants can be useful tools for modeling and analyzing carbon movements within a particular ecological system.

The Sonoran Desert Region contains many different biomes, however, for the purposes of this study, particular attention is given towards the desert biome (Dimmit, 2015). The desert biome of the Sonoran Desert exhibits an extremely arid climate, having natural water freely available usually only after major precipitation events. Studies estimate that Tucson has a

potential evapotranspiration (evaporation through water loss from plant leaves during photosynthesis) to precipitation ratio of 8:1, meaning that Tucson can evaporate approximately eight times more water than is actually supplied through rain events (Dimmit, 2015). Major rain events are seasonally characteristic, and occur in a bi-seasonal pattern. Between the months of December and March, frontal storms originating from the North Pacific are known to bring light winter rain events (Dimmit, 2015). In contrast, heavy monsoonal rain events occur during the summer between the months of July and mid-September. During this short period is when the Sonoran Desert receives most of its rainfall. However, while many plant species that live in this severely water limited ecosystem are highly adapted to doing so, they are not completely invincible to the high temperatures and extreme water shortages that continue to occur each year. As a result, water-stress can be a continuing challenge for plants endemic to the Sonoran Desert.

Regardless of location, all plants perform photosynthesis, or the process of converting carbon dioxide (CO_2), water (H_2O), and light energy into carbohydrate (glucose) and oxygen (O_2) products (i.e. $6CO_2 + 6H_2O$ + light energy $\rightarrow C_6H_{12}O_6 + 6O_2$). However, some plants employ different photosynthetic mechanisms than others. In general, trees and shrubs practice C_3 photosynthetic pathways, which is the most rudimental. C_3 photosynthetic systems use the Calvin cycle to fix atmospheric CO_2. In doing so, the highly inefficient process of photorespiration occurs as Rubisco reacts with O_2 instead of CO_2. In contrast, grasses are known to use C_4 photosynthetic pathways. This photosynthetic pathway is considered to be more efficient than the C_3 pathway because it is able to limit photorespiration by separating the processes of fixing atmospheric CO_2 and the Calvin Cycle.

To better understand the relationship between different photosynthetic pathways, carbon movement, and aridity stress, we analyzed leaf wax biomarkers in desert plants native to the Sonoran Desert. To represent a wide variety of plant life histories and growth patterns, we sampled the leaves of *Prosopis velutina* and *Olneya tesota* (two C_3 photosynthesizing tree species), *Simmondsia chinensis* (a C_3 photosynthesizing shrub species), and *Aristida ternipes* (a C_4 photosynthesizing grass species). *P. velutina*, commonly known as velvet mesquite, is a legume tree that is known to be highly drought tolerant. Their drought tolerance comes from a deep taproot system, however, 90% of their root system is located within the top 3ft of soil (Dimmit, n.d.). These plants have many small leaves that are able to close upon themselves during extreme heat to protect themselves from harmful solar radiation damage or excessive

drying out (Dimmit, n.d.). *O. tesota*, otherwise known as ironwood, is another legume tree that is nearly endemic to the Sonoran Desert (Hubbard, n.d.). This tree is known to grow at extremely slow rates, and simultaneously conducts low rates of photosynthesis in order to prevent excessive soil moisture loss. Due to their life history, ironwoods are ranked as one of the most drought tolerant Sonoran Desert plant species, particularly due to their profound water use efficiency (Hubbard, n.d.). *S. chinensis*, or jojoba, is an evergreen shrub species that has vertically positioned leaves, making this plant especially adapted to the Sonoran Desert's extreme heat. The vertical orientation of the leaves is helpful in reducing water loss, because the sun's radiation only reaches the edges of the leaves during the midday of the summer months, whereas, during the morning and late afternoon, the sun's radiation is more readily able to reflect onto the leaves' surface─a notably beneficial adaptation since temperatures are cooling during this time, and energy capture for photosynthetic processes is more favorable (Dimmit, n.d.) . Along with a specially adapted leaf structure, *S. chinensis* is also known to produce large concentrations of leaf waxes, which protect the plant's leaves from sun radiation and excessive water losses. Finally, *A. ternipes*, also known as spider grass, is a grass perennial grass found in the Sonoran Desert. Like many grasses, *A. ternipes* is highly responsive to precipitation events and is known to grow and flower in as little as 5 weeks after germination given 1.8 inches of rainfall (Van Devender & Dimmitt, n.d.).

Within the environment, the element carbon has three naturally occurring isotopes: ^{12}C, ^{13}C, and ^{14}C. Here, we focus on the two stable isotopes of carbon, ^{12}C and ^{13}C, because they are differently fractionated by photosynthetic pathways. Differences in isotope assimilation into the plant structure is mainly attributed to differences in the diffusion rates of $^{12}CO_2$ and $^{13}CO_2$ during photosynthetic assimilation of CO_2, in conjunction with carboxylation enzyme preference for one isotopic form of carbon dioxide over another (Monson & Baldocchi, 2014). Photosynthetic assimilations of CO_2 and carboxylation enzyme preference is dependent upon the photosynthetic mechanisms that each plant uses─either C_3 or C_4 in this case. In regards to C_3 plants, Rubisco enzymes demonstrate a large kinetic isotopic effect which favors the assimilation of $^{12}CO_2$ over $^{13}CO_2$. Rubisco favors $^{12}CO_2$ because reactions with this isotopic variation of CO_2 require lower activation energies to catalyze the reactions necessary for photosynthesis to occur. Thus, covalent bond formation and the resulting photosynthetic reactions are able to occur at faster reaction rates, giving $^{12}CO_2$ a preferential advantage for plants utilizing this photosynthetic

mechanism. However, $^{13}CO_2$ will still be used in C_3 photosynthetic mechanisms because it cannot be entirely discriminated against. This is because there will still be available $^{13}CO_2$ present within the atmosphere, and once inside the stomata, $^{13}CO_2$ exudes a high diffusive resistance, reducing a plants ability to biochemically discriminate against the assimilation of this isotopic compound (Monson & Baldocchi, 2014). On the other hand, C_4 plants use a more efficient photosynthetic mechanism, and therefore, the exclusion of $^{13}CO_2$ is not as pertinent. Regardless of pathway, both mechanisms exhibit a depletion of ^{13}C within the plant leaves, as they continue to discriminate against the heavier ^{13}C isotope. Thus, carbon isotopes have proven to be a useful tool in studying and monitoring plant metabolic pathways, and also help indicate the largest sources and sinks for biogeochemical processes (Monson & Baldocchi, 2014).

In addition to different isotopic compositions of carbon, there is also different long chain lengths (C_{21} to C_{37}) *n*-alkanes that act as terrestrial plant biomarkers. These long chain normal alkanes are created within the epicuticular leaf waxes of terrestrial plants and often indicate an odd-over-even predominance with one or two dominant chain lengths (Bush & McInerney, 2013). *n*-Alkanes are vital to analyzing plant life histories because these organic compounds act as the plant's first barrier from the external environment, and are known to protect the leaf from excessive water losses through evaporation (Bush & McInerney, 2013). The isotopic composition and concentration of leaf wax *n*-alkanes can also provide insight into how variations in leaf wax isotopic composition reflect adaptations or reactions to Sonoran Desert environmental pressures.

In this study, we measure the concentrations of leaf waxes as well as their distributions, as defined by the average chain length (ACL) and carbon preference index (CPI) metrics. ACL simply refers to the *n*-alkane chain length that shows up the most, where:

$$ACL = \Sigma (C_n \times n) / \Sigma (C_n),$$

where C_n refers to the concentration of each *n*-alkane and their *n* carbon atoms (Bush & McInerney, 2013). CPI, on the other hand, refers to the ratio of abundance of odd over even carbon number paraffins, and can defined as:

$$CPI = [\Sigma_{odd} (C_{21-33}) + \Sigma_{odd} (C_{23-35})] / (2\Sigma_{even} C_{22-34})$$ (Bush & McInerney, 2013).

We then analyze the $\delta^{13}C$ of the plant wax *n*-alkanes to study how carbon isotope fractionation differs by species and through the annual cycle.

METHODS

Leaf Sample Collection

Leaf samples were collected every month by Junior Docent volunteers from an unirrigated sector of the Sonoran desert just outside the grounds of the Arizona-Sonoran Desert Museum. Volunteers removed multiple leaves from at least 2 or 3 individual specimens using clean scissors. Collected sample mass varied, however, the average range in mass was between 0.300-1.20 grams. Samples were placed into labeled Whirl-Pak bags, and transported to the Tierney Organic Geochemistry Lab where they were stored in a freezer until sample analysis was ready to be conducted.

Leaf Sample Preparation using Freeze Dryer

Prior to freeze drying, samples were individually rinsed with deionized (DI) water to remove any possible dirt and debris that could contaminate the sample. Tweezers cleaned with methanol and dichloromethane were used to handle the samples. Post-rinsing, leaves were removed from their stems and placed back into a Whirl-Pak bag. Once all samples were rinsed, samples were placed into the Freeze Dryer to remove any remaining excess water. Samples were freeze dried at ~50˚C and 0.4mBar vacuum pressure for approximately 48 hours. Dried samples were then broken up inside their respective Whirl-Pak bags.

Lipid isolation using Accelerated Solvent Extraction

Prior to sample preparation, the ASE 350 was prepped. Solvent reservoir A was filled with 1600mL of DCM:MeOH (9:1) mixture to allow for a batch run of twenty four 22mL cells. To prepare the 22mL cells, a 27mm glass fiber filter was placed at the end of the cap and the barrel component of the cell was screwed into this cap. Special care was taken to ensure that the barrel did not catch any parts of the filter in the threading. A second 27mm glass fiber filter was then placed inside the barrel of the cell and pushed down using a precleaned (with DCM) black cylindrical tube. Even pressure was applied when doing so to ensure that the filter was inserted as evenly as possible to the bottom of the cell barrel.

The amount of sample needed for the extraction process varied between species. In general, 0.100 to 0.400 grams of *P. velutina*, 0.100 to 0.400 grams of *O. tesota*, 0.100 to 0.500 grams of *A. ternipes*, and 0.600 to 1.000 grams of *S. chinensis* were weighed out for the

extraction process. Mass ranges were determined using masses from previous batch runs conducted within the Tierney Organic Geochemistry Lab. To facilitate even lipid extraction, leaf samples were mixed with precombusted diatomaceous earth (DE). The exact mass of diatomaceous earth used was relative to each sample and depended upon how full the cell was with each sample, prior to the inclusion of DE. Samples were transferred into their respective ASE cell using an aluminum ASE cell funnel (precleaned with methanol and DCM between samples). Once the ASE cell was almost full, another 27mm glass fiber filter was placed at the top of the barrel. The black cylindrical tool (precleaned with DCM between samples) was used to press this filter into the barrel so it sat carefully above the sample and DE mixture. Approximately 4mm of empty space was left at the top of the cell. The cell cap was then placed onto the cell, and the cell was labeled with the sample's identifying label information. The following procedure was repeated for all samples within each batch (approximately 24 cells per batch). All materials used were cleaned between samples to prevent cross-contamination.

Cells were then loaded onto the upper carousel of the ASE 350 machine in their corresponding order. Precombusted and labeled collection vials were placed in the lower carousel to collect the solvent and lipid extract that percolates through and out of the cell during the extraction process. Samples were left to run on the ASE 350 machine overnight.

After successful extraction, collection vials were spiked with 200 µL of general recovery standard, containing a mixture of 5000ng of 5α-androstane and 5000ng of *cis*-11-eicosanoic acid, prior to Flexi-Vap evaporation (evaporation conducted using nitrogen). 5α-androstane standard was chosen because it elutes out in the aliphatic fraction during column chromatography separation. *cis*-11-eicosanoic acid standard was added for acid fraction analysis−though acid sample fractions were not analyzed within this study. Completely evaporated samples were then rehydrated with DCM:IPA (2:1) solvent, and transferred into 4mL vials. Using the Flexi-Vap samples were again blown down.

Due to their high concentration, samples were split in half. To do this, 2000µL of DCM:IPA was added to the 4mL vial. After appropriate mixing, 1000µL of sample was removed from the vial and placed into a separate 4mL vial labeled for permanent storage. The remaining 1000µL of sample and solvent mixture was blown down for column chromatography extraction.

Total Lipid Extract Separation using Two-Column Chromatography

Two-Column Chromatography extraction was used to separate the total lipid extracts within the samples. The first column chromatography extraction involved a LC-NH_2 gel column and its purpose was to separate the fatty acids within the sample from the rest of the lipids in the extract. The LC-NH_2 gel is used because the amine groups (-NH_2) strongly bond with the acid functional groups (-COOH) comprising the peptide bonds along the fatty acids. When loading the sample onto the column, DCM:IPA (2:1) solvent is used, which causes the acids in the extract to get stuck in the LC-NH_2 gel. However, the neutral lipids present within the sample will elute through the column. In the case of the first set of columns, this fraction represented the DCM:IPA fraction. After this fraction has eluted through the column, 4% acetic acid in DCM (a stronger acidic solvent) is used to release the acidic compounds from the LC-NH_2, for the solvent binds with the acetic acid, allowing the fatty acids to elute out, becoming the acid fraction. The acid fractions were archived and placed into storage.

A second column chromatography extraction was conducted using the DCM:IPA fraction to further separate the neutral fraction. This second column chromatography extraction involved a Si gel column. The neutral fraction was initially loaded onto the column using hexane. This eluted fraction was the "aliphatic fraction", and it contained all of the apolar aliphatic compounds, including alkane compounds. The sample was then loaded onto the column with a 70:30 mixture of Hexane:DCM (i.e. 30% DCM in hexane). The remaining eluted fraction was referred to as the "aromatic fraction", for it contained the aromatic compounds, including alkenones and ketones, of the lipid sample. After this second column, all of the lipid extracts were separated into their constituent organic compounds. For the purpose of this study, the aliphatic fraction was of interest, as it contained the alkane biomarkers.

For further analysis, the aliphatic fraction was transferred into 2mL V-vials using hexane. Samples were then blown down under the Flexi-Vap using nitrogen.

Alkane Concentration Determination using GC-FID

Aliphatic fractions were ran on a Thermo-Scientific TRACE 1310 Gas Chromatograph-Flame Ionization Detector (GC-FID) to determine the concentrations of alkanes present within each sample, relative to the internal standard. A 30m DB-5 column was used with a 0.32mm internal diameter and 0.25μm film. To analyze the samples, each sample was rehydrated with varying μL amounts of hexane (rehydration volumes were dependent upon calculated

concentration and dilution levels). A sample volume of 1µL was injected into the GC-FID's Programmable Temperature Vaporizing (PTV) inlet at a temperature of 60˚C. Injected sample was held for 0.1 minutes to vaporize the hexane solvent, and then ramped up to 325˚C (temperature increase rate of 10˚C/minute) to vaporize the remaining sample. Oven initial temperature was 60˚C, and vaporized sample was held for 2 minutes. A remaining two oven ramps were performed: one at 170˚C (temperature increase rate of 20˚C/minute) to remove C_6 through C_{18} *n*-alkane carbon chains, and another at 325˚C (temperature increase rate of 8˚C) to slowly separate remaining *n*-alkane carbon chain peaks for further analysis. Peak areas for each sample were calculated using MatLab computer software. Peak areas were compared against the 5a-androstane internal standard to calculate concentrations. ACL and CPI were determined using the ACL and CPI equations defined above.

Mean $\delta^{13}C$ ratio Determination using GC-IRMS

Aliphatic fractions were ran on a Thermo-Scientific Delta V Plus Gas Chromatograph-Isotope Ratio Mass Spectrometer (GC-IRMS) to determine mean $\delta^{13}C$ ratios, normalizing data to VPDB reference standards. A6 standard was ran alongside aliphatic fractions to monitor drift and offsets. Precision of the measurements was 0.2‰ or better.

RESULTS

Concentrations of n-Alkanes, ACL, and CPI

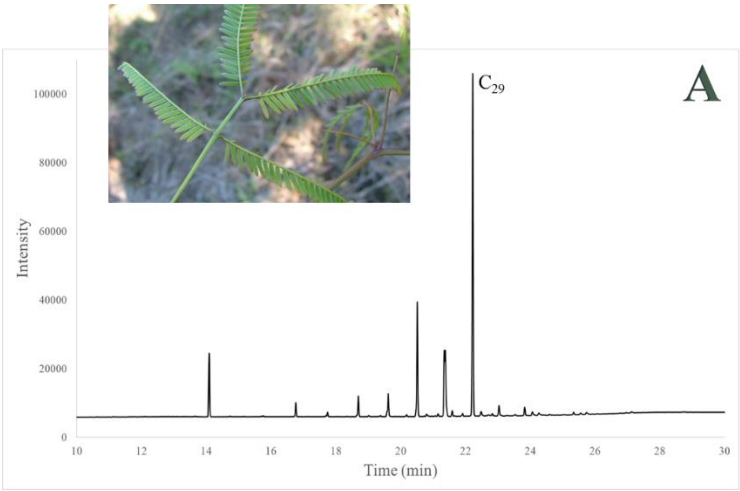

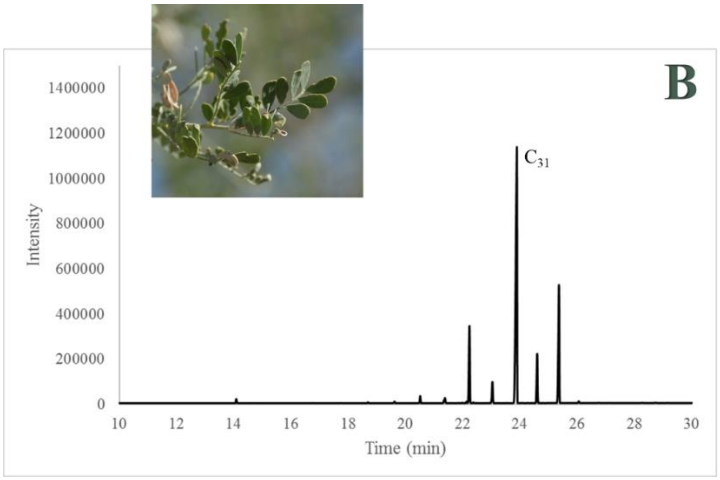

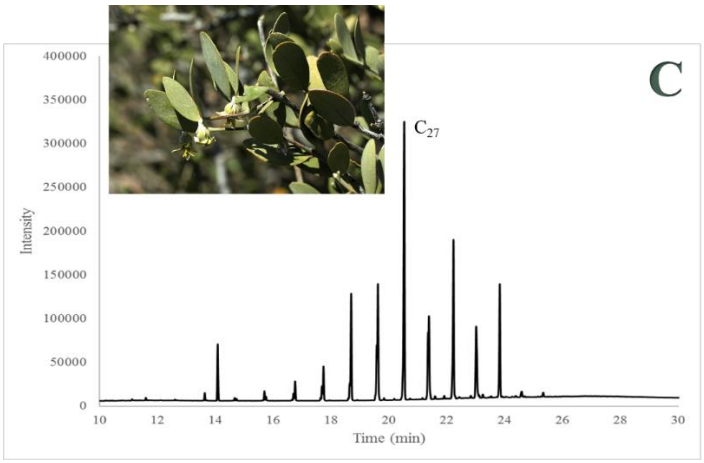

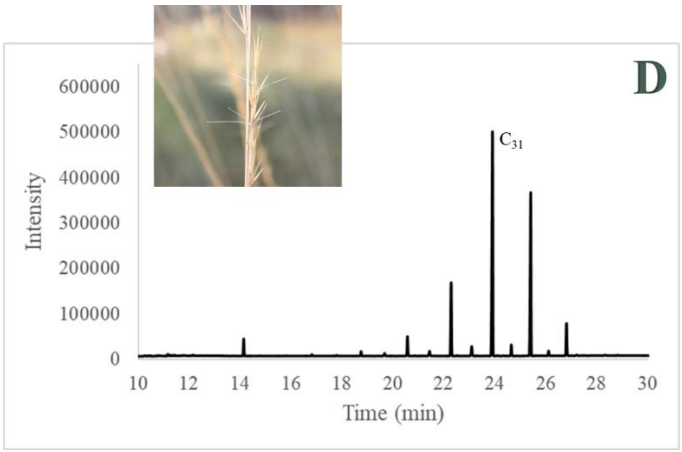

Figure 1. Example GC-FID chromatograms for four Sonoran Desert plant species. Highest peaks are denoted with their associated carbon chain length. (A) *Prosopis velutina* (velvet mesquite), (B) *Olneya tesota* (ironwood), (C) *Simmondsia chinensis* (jojoba), and (D) *Aristida ternipes* (spidergrass).

GC-FID chromatograms for each species indicate the long *n*-alkane chain lengths present within each aliphatic fraction sample. The peak with the highest intensity reflects the most abundant *n*-alkane chain for each plant species.

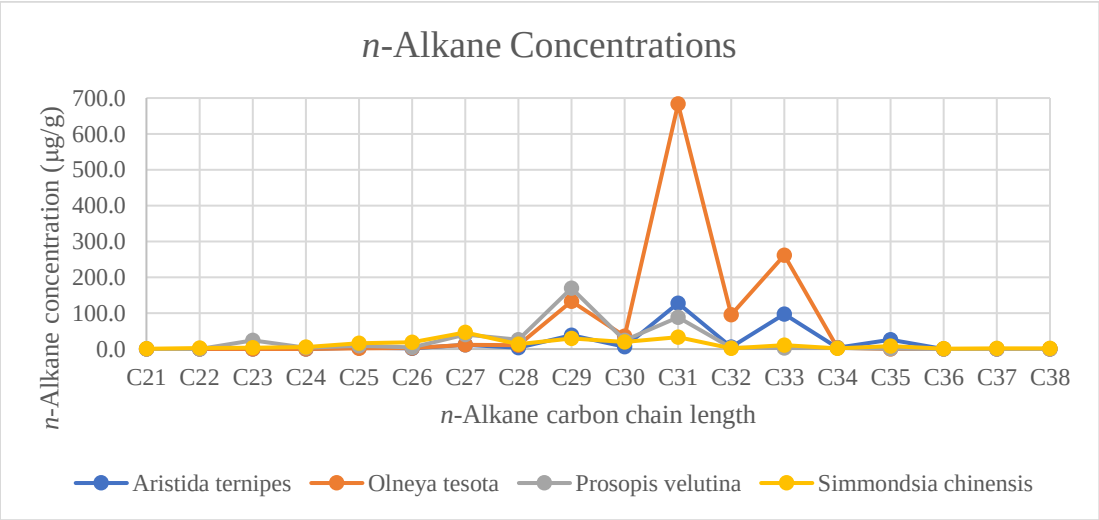

Figure 2. Average *n*-alkane concentrations for four Sonoran Desert plant species. Some data is omitted for *P. velutina* and *O. tesota* due to possible sample mislabeling.

Average *n*-alkane concentrations indicate the most abundant *n*-alkane chain present within each plant species. Most abundant *n*-alkane chains are the following: C_{27} for *S. chinensis*, C_{29} for *P. velutina*, C_{31} for *A. ternipes*, and C_{31} for *O. tesota*. For further comparison purposes, C_{29} was used for *S. chinensis* even though C_{27} was actually the most abundant homolog.

Data omissions for *P. velutina* and *O. tesota* are due to mislabeling events that occurred somewhere along the two-column separation process. Mislabeling was recognized during GC-FID sample peak analysis, and was further confirmed with GC-IRMS peak analysis. Mislabeled samples were omitted from the remainder of the study.

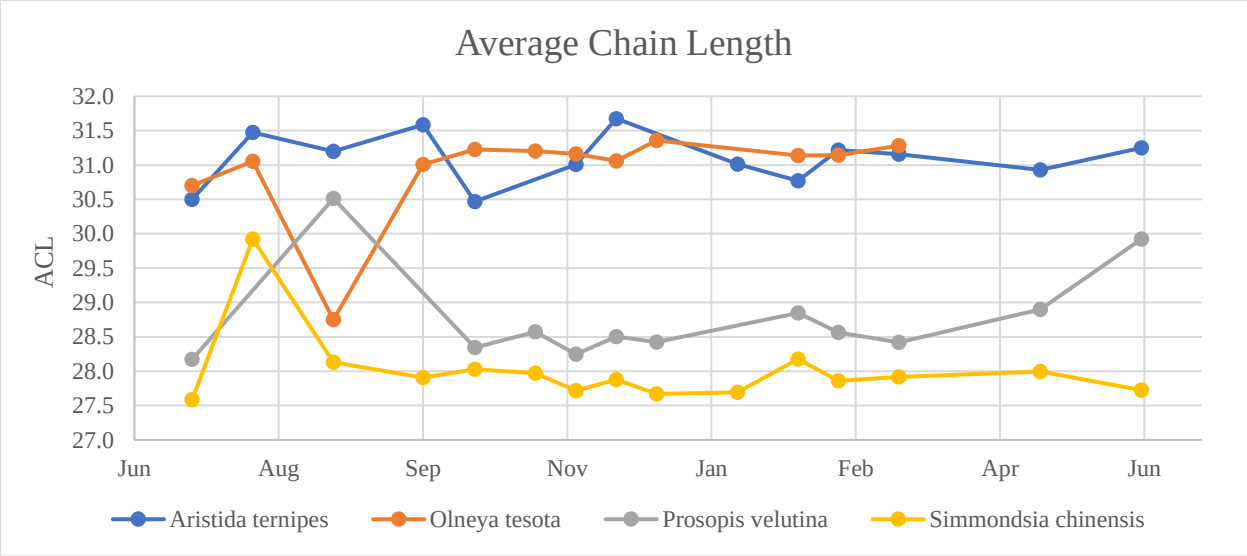

Figure 3. Average Chain Length for four Sonoran Desert plant species. Some data is omitted for *P. velutina* and *O. tesota* due to possible sample mislabeling.

C_3 plant leaf waxes have ACL values roughly ranging between 27.5 and 31.5. Specific species ACL ranges for C_3 plant species are the following: 27.6 to 29.9 (mean of 28.0) for *S. chinensis*, 28.2 to 30.5 (mean 28.8) for *P. velutina*, and 28.8 to 31.4 (mean 30.9) for *O. tesota*. C_4 plant leaf waxes have ACL values generally ranging between 30.5 and 31.75. Specific ACL ranges for *A. ternipes* are 30.5 to 31.7 (mean 31.10).

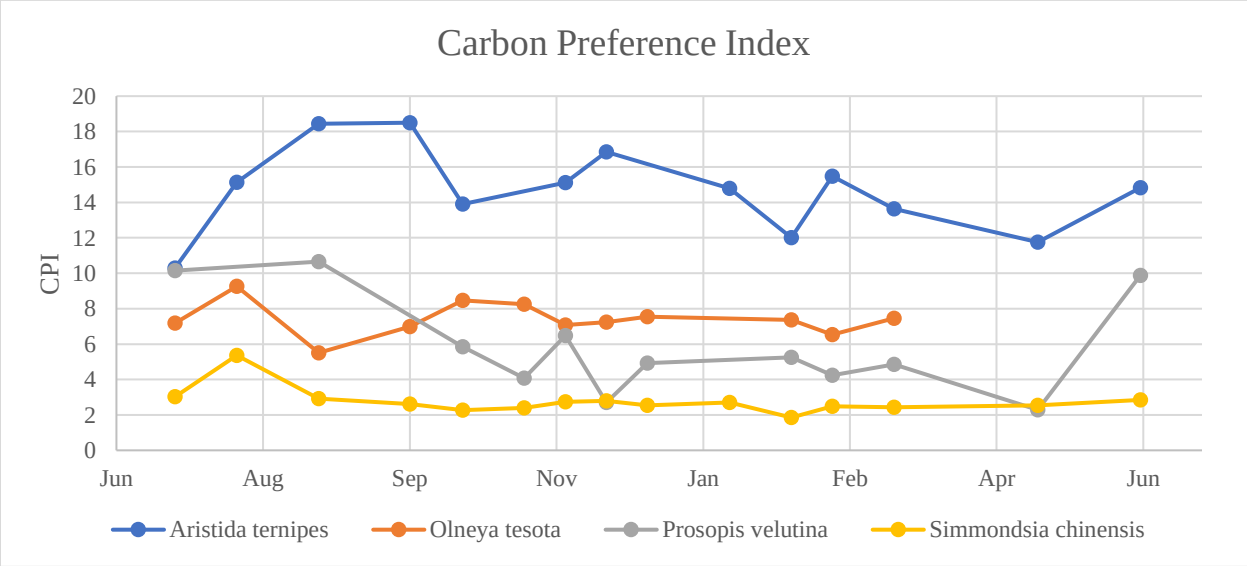

Figure 4. Carbon Preference Index for four Sonoran Desert plant species. Some data is omitted for *P. velutina* and *O. tesota* due to possible sample mislabeling.

C_3 plant leaf waxes have CPI values roughly ranging between 1.75 and 11.0. Specific species CPI ranges for C_3 plant species are the following: 1.85 to 5.40 (mean of 2.77) for *S. chinensis*, 2.29 to 10.7 (mean 5.94) for *P. velutina*, and 6.53 to 9.30 (mean 7.41) for *O. tesota*. C_4 plant leaf waxes have CPI values generally ranging between 10 and 19. Specific CPI ranges for *A. ternipes* are 10.3 to 18.5 (mean 14.68).

$\delta^{13}C$ Anomalies and Major Rainfall Events

Date	Precipitation (in.)
July 17, 2016	0.25
July 20, 2016	0.12
July 27, 2016	0.12
July 28, 2016	0.41
July 29, 2016	0.86
July 31, 2016	0.70
August 9, 2016	0.86
November 3, 2016	0.40
January 21, 2017	0.24
January 23, 2017	0.13

Table 1. Archived Tucson International Airport precipitation event measurements.

In addition to the leaf wax results described below, archived precipitation data from the Tucson International Airport station were acquired to analyze the relationship between precipitation and mean $\delta^{13}C$ anomalies. Precipitation events were only recorded if there was a measured amount of rain higher than 0.10 inches.

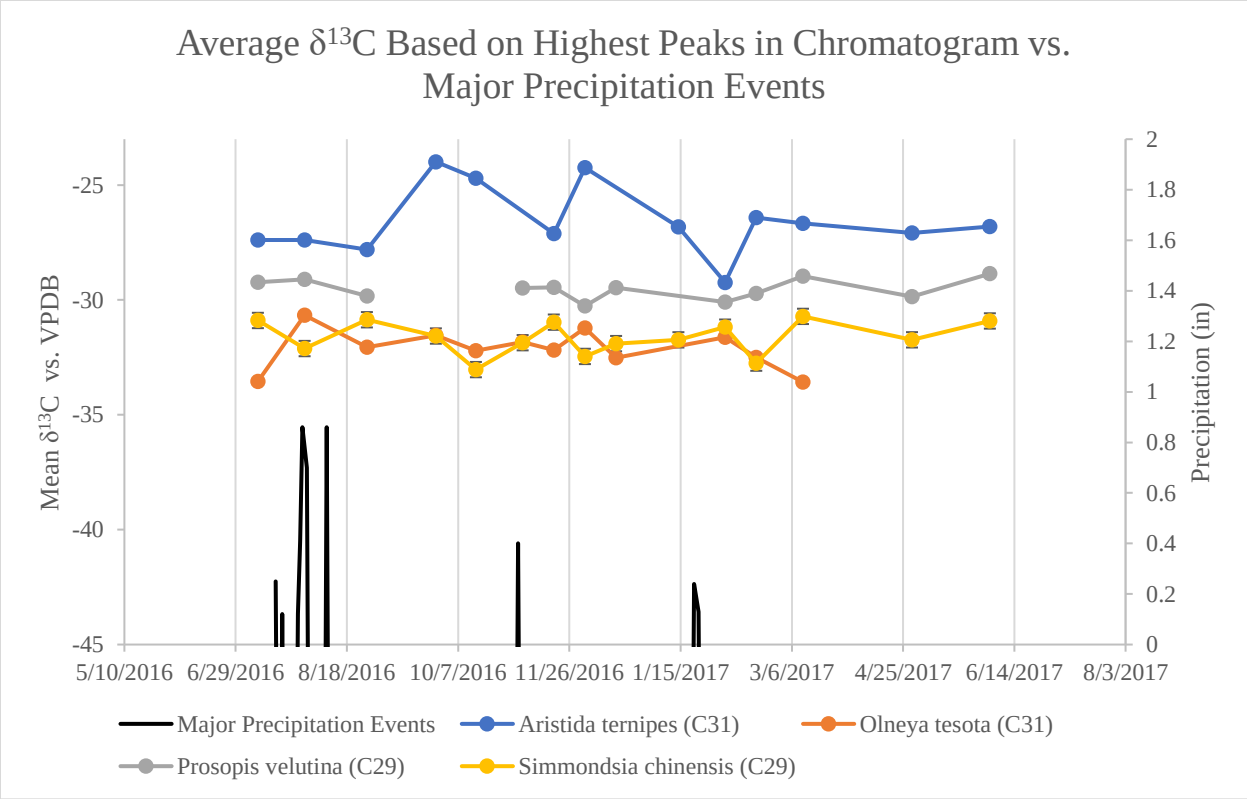

Figure 5. Mean $\delta^{13}C$ ratios in relation to major precipitation events for four Sonoran Desert native plant species. Major precipitation events reflect rain events detailed in Table 1. $\delta^{13}C$ are determined on the most abundant *n*-alkane for each species. Error bars indicate mean standard deviations for the highest peaks of each species. For comparison purposes, C_{29} is used for *S. chinensis* even though C_{27} was actually the most abundant homolog. Some data is omitted for *P. velutina* and *O. tesota* due to possible sample mislabeling.

C_3 plant leaf waxes have $\delta^{13}C$ values ranging from -34 to -40‰ (mean of -37‰) (Monson & Baldocchi, 2014). Our results indicate that all three C_3 plants (*P. velutina*, *O. tesota*, and *S. chinensis*) fall within this range. C_4 plant leaf waxes have $\delta^{13}C$ values ranging between -20 to -26‰ (mean of -22.5‰) (Monson & Baldocchi, 2014). *A. ternipes* results mostly coincide with this range.

DISCUSSION

Concentrations of n-Alkanes, ACL, and CPI

Plant leaf waxes are known to contain many different types of organic components within its structure. In regards to *n*-alkanes within the plant leaf waxes, results indicate a great variation in the concentrations and abundances of *n*-alkanes per grams of leaf sample, even between plant

species of similar photosynthetic mechanisms. For instance, *O. tesota*, a C_3 plant species, leaf waxes contain significant concentrations of *n*-alkane chains, whereas *S. chinensis*, also a C_3 plant species, contains very little concentrations of *n*-alkanes within their leaf waxes. *S. chinensis*' trend of lower *n*-alkane concentrations could be attributed to a preference for making another type of wax that is more concentrated in another functional groups, rather than the relative alkanes. In contrast, *O. tesota*'s dominance in *n*-alkane carbon concentration could be attributed to the leaves' highly adaptive water conservation capabilities, which may be assisted by the presence of high *n*-alkane concentrations within the leaf wax, though this will need to be further investigated. Differences between *n*-alkane concentrations of similar plant types was also represented by the results, for *P. velutina* and *O. tesota* are both legume tree species, however, *P. velutina* shows a carbon-number maxima (C_{max}) of C_{29} and *O. tesota* shows a strong concentration preference towards C_{31}. Differences in concentrations and preferred C_{max} values could also be attributed to different plant life histories, as *O. tesota* is known for its extremely slow growth rates and water conservation, whereas *P. velutina* contains many smaller leaves that do not conserve water to the same degree. Finally, *A. ternipes* demonstrates greater concentrations of longer *n*-alkane chain lengths (C_{31}-C_{35}), which may be attributed to the plants C_4 photosynthetic mechanisms in relation to the Sonoran Desert's arid environment, however, this relationship is still poorly understood (Bush & McInerney, 2015).

In regards to general abundances, all plant species tend to produce a higher amount of odd-number carbon chains over even-number carbon chains. However, *S. chinensis* is again an outlier, for the degree of this trend is much less significant. The inclusion of many more even-number carbon chains than other species could be attributed to the species' lower concentration of *n*-alkanes in contrast to all other plant species, though again, this trend needs to be further investigated.

All species indicate seasonal variations within ACL and CPI, however, these seasonal variations are not consistent between species. ACL results (Figure 3) vary between species, including between C_3 and C_4 plant species. *S. chinensis* indicate a jump in preference towards longer *n*-alkane chain lengths throughout the summer season, though as the fall and winter seasons commence, ACL moves towards a general stabilization around 27.75. Similar to *S. chinensis*, *P. velutina* demonstrates an increase in the concentration of longer *n*-alkane chain lengths during the summer months, though the severity of this increase is difficult to assess, as

two sampling dates are omitted due to sample mislabeling. Approaching the fall and winter months, *P. velutina* ACL demonstrates a rough stabilization around 28.5, and then as summer nears again, ACL values increase again. *O. tesota* demonstrate a general preference for longer *n*-alkane chains, in comparison to the other C_3 plant species, *S. chinensis* and *P. velutina*. A large trough, or decrease in the concentration of longer *n*-alkane chains within the leaf wax, is shown briefly during the summer. Stabilization of *O. tesota n*-alkane chain lengths, average of 31.25, was maintained throughout the fall and winter seasons. Spring season trends cannot be assessed at this time, due to omission of mislabeled samples. *A. ternipes* demonstrates the greatest overall seasonal variability in ACL. ACL averages around 31.0 for the annual year, however, reductions in *n*-alkane chain length concentrations are observed to occur during the beginning of the fall and spring seasons.

CPI results (Figure 4) show variable changes throughout the annual cycle. Overall, *S. chinensis* demonstrates a tendency towards lower CPI, or a lower ratio of abundance of odd over even number carbon paraffins, in comparison to all other analyzed plant species. A small increase in CPI can be seen towards the end of June, or the end of the monsoon season, however, *S. chinensis* drops to 2 and remains around this value for the rest of the annual cycle. Throughout the annual cycle, *P. velutina* shows strong increases in CPI during the summer months and a declining trend during the remaining seasons. Therefore, results indicate *P. velutina* has a preference for producing odd carbon number *n*-alkanes in their leaf wax structures over even carbon numbers during the summer seasons. *O. tesota* indicates an average annual CPI of 7, though CPI varies during the summer season. CPI stabilization occurs back around 7, with the nearing of the fall and winter seasons. In regards to all species, *A. ternipes* not only indicates the strongest overall predominance of odd carbon number *n*-alkanes over even carbon number *n*-alkanes, but also the greatest seasonal variability in CPI, as well.

Additionally, variations in ACL and CPI do not reflect to be attributed to major rain events for any of the plant species, as there is no general behavioral trend in association with these events. Looking further into plant responses to temperature and the incorporation of mislabeled data may assist with the interpretation of these trends and may shed light onto the influences of environmental stresses that are not apparent at this point in time.

$\delta^{13}C$ Anomalies and Major Rainfall Events

$\delta^{13}C$ represents the ratio of $^{13}C/^{12}C$. Most C_3 plants have $\delta^{13}C$ values ranging from -24 to -30‰ (mean of -27‰) because Rubisco processes favor ^{12}C, and discriminate against ^{13}C whenever possible. Usually C_4 plant $\delta^{13}C$ values range between -10 to -16‰ (mean of -12.5‰). However, leaf wax $\delta^{13}C$ values are roughly offset by an additional -10‰, coinciding with the result data (Rommerskirchen et al., 2006) (Vogts et al., 2009). Despite the offset, C_3 plants were shown to be more depleted in ^{13}C than ^{12}C, validating the hypothesis that plants using different photosynthetic pathways will display different fractionation behaviors in response to seasonally changing environmental conditions.

In general, less negative $\delta^{13}C$ anomalies indicate higher ^{13}C enrichment (lower depletion in ^{13}C); whereas, more negative $\delta^{13}C$ anomalies indicate greater ^{13}C depletion (lower enrichment in ^{13}C). In other words, a less negative $\delta^{13}C$ anomaly indicates that a plant is less depleted in ^{13}C, meaning the plant's stomata are unable to preferentially discriminate against ^{13}C for ^{12}C. Less negative $\delta^{13}C$ anomalies can occur when plants are water-stressed, as they tend to sacrifice photosynthetic ^{12}C fractionation preference for water conservation. Due to water-stresses, the plant only opens its stomata for brief periods of time, which forces the plant to accept any isotopic variation of carbon present within the surrounding atmosphere; therefore, resulting in a loss of preferential fractionation. The opposite is true for less water-stressed plants, resulting in more negative $\delta^{13}C$ anomalies, as their stomata are open for more extending periods of time, allowing for preferential ^{12}C fractionation to occur. Figure 5 results depict troughs shortly following 10 major precipitation events, which may indicate rain's assistive role in alleviating plant stress and allowing plants to preferentially fractionate ^{12}C. Less dramatic troughs throughout the monsoon season indicate a smaller response by plants to rain events and their respective carbon isotope fractionation. This is thought to be caused by a reduced water-stress state and increased photosynthetic activity. While the plants are receiving more water, they are also performing higher rates of photosynthesis, resulting in high losses of water. This period of time is also one of the hotter times of the year for plants. Therefore, a threshold is reached during this seasonal period, allowing for a balance between high photosynthetic rates and low water-stress. The stable threshold is only circumvented when multiple rain events of greater than 0.40 inches occurs (a significant amount of rainfall for this region). However, when the monsoon season ends, water-stress increases in the plants and their ability to preferentially fractionate ^{12}C

is seen to decrease again. The larger troughs seen in the winter and spring months are thought to occur because the plants are more heavily water-stressed, and therefore, any little amount of rain will significantly assist in alleviating water deficiencies.

In regards to specific species trends, *A. ternipes* is thought to demonstrate the greatest response to rain events because its shallow root system is able to quickly access precipitation infiltrating the desert soil surface. *P. velutina* is theorized to be "immune" to rain events because of its large taproot system. *O. tesota* and *S. chinensis* express similar but alternating responses to seasonal changes and precipitation events, while simultaneously maintaining relatively constant $\delta^{13}C$ anomalies. Possible explanations for this could be that *O. tesota* is ranked as one of the Sonoran Desert's best plants at conserving water, which could possibly explain its relative stability throughout the annual cycle. *S. chinensis*, on the other hand, is known to produce a thick wax coating on its leaves. This thicker than normal leaf wax might explain why *S. chinensis* demonstrates greater delays in its ability to preferentially fractionate, as the thick waxy coating limits the amount of sun stress that the plant experiences, decreasing the degree of water-stress that the plant experiences.

While it is important to understand how $\delta^{13}C$ anomalies can assist with determining the occurrence of major rain events, they do not specify where the rain is coming from. As a result, further research investigating deuterium anomalies may be a promising solution to further analyze how annual climatic variations and monsoonal precipitation in the Sonoran Desert affect plant development and life history cycling.

CONCLUSION

n-Alkanes as terrestrial plant biomarkers have proven to be highly beneficial when investigating environmental stresses and their effects on both plant leaf wax development and plant life histories. However, this study is one of the first-known studies to investigate *n*-alkane distributions and carbon isotopic preference in Sonoran Desert native species. This study finds that seasonality along an annual cycle influences *n*-alkane distributions and carbon isotope anomalies, though the roles of specific environmental stressors within these seasons must be further investigated to more definitively determine the implications of seasonality on Sonoran Desert plant life histories. Nevertheless, surprising results did arise from this study.

One of such surprises is the distribution of *n*-alkanes within the *S. chinensis* leaf wax. In comparison to the other analyzed species, results indicated that *S. chinensis* produces less alkanes despite its life history of nominally producing more leaf waxes overall. While this respective difference in *n*-alkane distribution is most likely attributed to *S. chinensis* producing different waxes than *n*-alkanes in larger concentrations, it provides evidence for the preference of plants to produce one form of leaf wax over another.

In regards to carbon-isotope anomalies, our results indicate that there may not be as large of a spread distribution between C_3 and C_4 plants as we previously anticipated. For example, A. *ternipes* was overall more enriched in $\delta^{13}C$ than the other plant species. While a higher enrichment was expected for this C_4 plant, we did not anticipate such a small spread in enrichment between this species and the other C_3 species. Previous literature (Rommerskirchen et al., 2006) (Vogts et al., 2009) indicate enrichment differences between C_4 and C_3 species to be approximately 10‰, whereas our results demonstrate only a 2‰ difference (in regards to *A. ternipes* and *P. velutina*). Additionally, *A. ternipes* has an average $\delta^{13}C$ anomaly around -26.6‰, which extends out of the expected range for C_4 plant leaf wax $\delta^{13}C$ anomalies (average of -22.5‰). In contrast, all of the C_3 plants have average $\delta^{13}C$ anomalies that are greater than the minimum expected range of C_3 plant leaf wax $\delta^{13}C$ anomalies (average of -37.0‰). Thus, the smaller separation in $\delta^{13}C$ anomalies between C_3 and C_4 plant species may serve as a possible implication for future understandings of how Sonoran Desert plants are fixing carbon specifically within this arid environment.

Finally, this study demonstrated that $\delta^{13}C$ anomalies may be useful tools in demonstrating how the occurrences of major rain events, or other environmental stressors, can affect or even alter Sonoran Desert plants' ability to fix carbon. While implications of these results are still very broad, this could prove to be a useful tool in monitoring environmental stress effects within the Sonoran Desert region.

ACKNOWLEDGEMENTS

Special thank you to Dr. Jessica Tierney for her wise counsel and supervision throughout this project, as well as, Patrick Murphy for his continuous support and teaching within the lab.

REFERENCES

Bush, R. T., & McInerney, F. A. (2013, April 29). Leaf wax n-alkane distributions in and across modern plants: Implications for paleoecology and chemotaxonomy. *Geochimica et Cosmochimica Acta*, 161-179.

Bush, R. T., & McInerney, F. A. (2015). Influence of temperature and C4 abundance on n-alkance chain length distributions across the central USA. *Organic Geochemistry*, 65-73.

Clark, I., & Fritz, P. (1997). *Environmental Isotopes in Hydrology.* CRC Press.

Collister, J. W., Rieley, G., Stern, B., Eglinton, G., & Fry, B. (1994). Compoud-Specific δ13C analyses of leaf lipids from plants with differing carbon dioxide metabolisms. *Organic Geochemistry, 21*, 619-627.

Diefendorf, A. F., & Freimuth, E. J. (2016, October 22). Extracting the most from terrestrial plant-derived n-alykl lipids and their carbon isotopes from the sedimentary record: A review. *Organic Geochemistry*.

Diefendorf, A. F., Freeman, K. H., Wing, S. L., & Graham, H. V. (2011, September 22). Production of n-alkyl lipids in living plants and implications for the geologic past. *Geochimica et Cosmochimica Acta*, 7472-7485.

Dimmit, M. A. (2015). Biomes and Communities of the Sonoran Desert Region. In M. A. Dimmitt, P. W. Comus, & L. M. Brewer, *A Natural History of the Sonoran Desert* (2nd ed., pp. 5-20). Arizona-Sonora Desert Museum Press & University of California Press.

Dimmitt, M. A. (n.d.). *Fabaceae (legume family)*. Retrieved from Arizona-Sonora Desert Museum: https://www.desertmuseum.org/books/nhsd_fabaceae.php

Dimmitt, M. A. (n.d.). *Simmondsiaceae (jojoba family)*. Retrieved from Arizona-Sonora Desert Museum: https://www.desertmuseum.org/books/nhsd_simmondsiaceae.php

Hubbard, T. (n.d.). *Biological Survey of Ironwood Forest National Monument: Natural History of the Desert Ironwood Tree (Olneya tesota)*. Retrieved from Arizona-Sonora Desert Museum: https://www.desertmuseum.org/programs/ifnm_ironwoodtree.php

Monson, R., & Baldocchi, D. (2014). *Terrestrial Biosphere-Atmosphere Fluxes.* Cambridge University Press.

Nelson, D. B., Knohl, A., Sachse, D., SchefuB, E., & Kahmen, A. (2016, November 16). Sources and abundances of leaf waxes in aerosols in central Europe. *Geochimica et Cosmochimica Acta*, 299-314.

Rommerskirchen, F., Plader, A., Eglinton, G., Chikaraishi, Y., & Rullkotter, J. (2006, April 27). Chemotaxonomic significance of distribution and stable carbon isotopic composition of long-chain alkanes and alkan-1-ols in C4 grass waxes. *Organic Geochemistry*, 1303-1332.

Sache, D., Billault, I., Bowen, G. J., Chikaraishi, Y., Dawson, T. E., Feakins, S. J., . . . Kahmen, A. (2012, January 4). Molecular Paleohydrology: Interpreting the Hydrogen-Isotopic Composition of Lipid Biomarkers from Photosynthesizing Organisms. *Annual Review of Earth and Planetary Sciences*, 221-249.

Van Devender, T. R., & Dimmitt, M. A. (n.d.). *Desert Grasses*. Retrieved from Arizona-Sonora Desert Museum: https://www.desertmuseum.org/books/nhsd_grasses.php

Vogts, A., Moossen, H., Rommerskirchen, F., & Rullkotter, J. (2009, July 23). Distribution patterns and stable carbon isotopic composition of alkanes and alkan-1-ols from plant waxes of African rain forest and savanna C3 species. *Organic Geochemistry*, 1037-1054.

Wunderground. (n.d.). *Weather History for KTUS*. Retrieved from WU: https://www.wunderground.com/history/airport/KTUS/2018/4/28/MonthlyCalendar.html?req_city=Tucson&req_state=AZ&reqdb.zip=85706&reqdb.magic=4&reqdb.wmo=99999#calendar